

Determination of a distribution of relaxation frequencies based on experimental relaxational data

C. J. Dias

Universidade Nova de Lisboa, Faculdade de Ciências e Tecnologia, Física Aplicada, Torre, 2825 Monte da Caparica, Portugal

(Received 6 November 1995)

A possible explanation for the relaxation behavior of many phenomena, and in particular of dielectric polarization phenomena, has been to assume the existence of a distribution of relaxation frequencies instead of a single relaxation frequency. It has been demonstrated that the natural scale for the distribution of relaxation frequencies is logarithmic in frequency axis. This assertion should be valid provided that there is both a relationship, between the frequency and the activation energy, of an exponential type like in an Arrhenius equation, and that a distribution exists in the domain of activation energies. These activation energies could possibly correspond to the energy states of the relaxing entities. A theory is then here presented to show that the product of the elapsed time by the depolarization current is a convolution of the distribution function of relaxation frequencies by a weight function of an asymmetric bell shape. A similar relationship is also shown to exist for the permittivity of a dielectric. Various consequences can be deduced from this theory, among them the determination of a similar relationship to that of the Hamon approximation. In the second part of this paper a deconvolution procedure has been proposed to find the distribution function of relaxation frequencies from experimental data, based on the above theory. Tests for this deconvolution procedure and its associated theory are reported, based on theoretical distribution functions as well as on data taken from previous published work. [S0163-1829(96)00321-9]

INTRODUCTION

The relaxation of polarization

The relaxation behavior in many systems (i.e., physical, biological, chemical, etc.) where a quantity P brought out of equilibrium relaxes toward its equilibrium value, can be described by a first-order differential equation such as

$$\frac{1}{\nu_d} \dot{P}(t) + P(t) = \lim_{t \rightarrow \infty} P(t), \quad (1)$$

where $1/\nu_d$ is the relaxation time or ν_d is the relaxation frequency. The equilibrium value of P will depend in general on the magnitude of the driving excitation. In this paper we will be interested in the phenomena of dielectric polarization and thus P will denote the polarization of the material.

Debye relaxation: The time and frequency domain

In the context of the linear dielectric theory the above type of equation bears the name of Debye relaxation and ν_d is then the relaxation frequency of a particular type of dipole moment.¹ In general, for a material exhibiting different types of dipole moments each of these have a characteristic relaxation frequency. From the study of the relaxation dynamics one can get therefore an insight on the various mechanisms of polarization present in the material under investigation.

In real materials however, it is a common finding that the relaxation for a particular type of dipole moment proceeds as if, rather than a single relaxation frequency, a distribution of relaxation frequencies characterized by a mean value and a standard deviation²⁻⁴ exists. Qualitatively, the mean value of this distribution should be linked to the inertia of the relaxing

dipole moment, while the standard deviation can be associated to the degree of interaction and/or disorder between the relaxing entities. We stress that this approach, of the distribution function of relaxation frequencies, should be regarded as one interpretation of the experimental data that is, by no means, the only possible one.¹⁶

The dynamic behavior for the relaxation of the polarization can be probed equivalently either in the time or in the frequency domain. In the time domain, one usually measures the change in polarization with time (i.e., the current). This experiment is carried out by applying a voltage V_0 to the sample for a sufficiently long time $t_p \gg 1/\nu_d$, so that the sample acquires a polarization P_0 . P_0/V_0 is then the total polarization charge which can be ascribed to the above dipole moment for each unit of the applied voltage. After performing the polarization, the voltage is switched off while the current (i.e., the change in polarization) is recorded during a time t_r , such that $t_r \ll t_p$. In the case of a Debye relaxation the current is

$$I(t) = \frac{dP(t)}{dt} = -\nu_d P_0 \exp(-\nu_d t) \quad (2)$$

corresponding to the following *relaxation function* of the polarization:

$$P(t) = P_0 \exp(-\nu_d t), \quad (3)$$

where the equilibrium value for the depolarization experiment was set to zero due to the absence of a driving voltage. Alternatively, in the frequency domain one measures the frequency dependence of the relative permittivity (in the fore-

going relative permittivity is shortened to permittivity unless stated otherwise) $\epsilon^*(\omega)$, which for a Debye relaxation is given by

$$\epsilon^*(\omega) - \epsilon_\infty = \frac{\epsilon(0) - \epsilon_\infty}{1 + i\omega/\nu_d} = \frac{\epsilon_s}{1 + i\omega/\nu_d}, \quad (4a)$$

where ϵ_∞ and $\epsilon(0)$ are the infinite and the static permittivity, respectively, while ω is the angular frequency, and ϵ_s is what will be called the relaxation strength of the dipole moment. This latter quantity is related to P_0/V_0 through

$$\epsilon_s = \epsilon(0) - \epsilon_\infty = P_0/(V_0 C_0), \quad (4b)$$

where C_0 is the geometric capacitance of the sample.

A quantity P_i , normally referred to as the instantaneous polarization, has not been mentioned above both because it is not linked to a dipolar relaxation mechanism, and its time constant is much shorter than the relaxation time of dipolar relaxation. P_i though is related to the infinite permittivity ϵ_∞ through $\epsilon_\infty = P_i/(V_0 C_0)$.

Kohlrausch-Williams-Watts relaxation function

In order to account for the experimentally found deviation from the Debye behavior various modifications of the polarization relaxation function [Eq. (3)] have been proposed, the most notable of which is the Kohlrausch-Williams-Watts (KWW) function,^{5,6}

$$P(t) = P_0 \exp[-(\nu_k t)^{\beta_k}], \quad (5)$$

where ν_k is the relaxation frequency and β_k is a parameter between zero and one. The latter parameter is qualitatively associated to the degree of interaction, between the relaxing entities, being closer to zero for strongly interacting dipole moments and to one for noninteracting ones.

Kubo relations

Kubo^{1,7} has derived some of the properties for the polarization relaxation function based on the fact that the value of the polarization relaxation for time t should equal the time average of its autocorrelation around the same time t . In this respect it should be noted that both the Debye and the KWW equations do not obey *all* of those properties, namely, that the odd derivatives of the relaxing polarization should be null for $t=0$,¹ provided the medium is thermodynamic equilibrium, i.e.,

$$P^{(2n+1)}(t=0) = 0. \quad (6)$$

Thus, the depolarization current at $t=0$ should equal zero, which is clearly not the case for the Debye relaxation function.

Kramers-Kronig relations

The real and imaginary parts of the permittivity are not independent of each other. In fact, in the frequency domain, a relaxation can be detected either as a peak in the imaginary part of the permittivity or as an inflexion in the curve of its real part. Formally, the equations connecting these quantities are known as the Kramers-Kronig relations.⁸

Relationship between dielectric constant and relaxation current

As was pointed out above there is an equivalence between the frequency and the time domain measurements. It is thus a matter of experimental convenience to make measurements in either domain. That is the main reason why low-frequency measurements (≤ 1 MHz) are usually performed in the time domain, while high-frequency measurements (≥ 0.01 Hz) are performed in the frequency domain. There is potentially a region of overlap which could be used to adjust the data from both domains.

Another reason to make low-frequency measurements in the time domain through depolarization current measurements is the fact that the dc conductivity also contributes to the imaginary part of the permittivity according to $\sigma_{dc}/i\omega$, increasing its value as the frequency decreases. In the low-frequency range, this contribution can be very large thus completely masking its dynamical behavior.

Formally the relationship between the relaxation function and the dielectric constant is given by⁹

$$\epsilon^*(\omega) - \epsilon_\infty = - \int_0^\infty \frac{I(t)}{C_0 V_0} e^{i\omega t} dt. \quad (7)$$

This expression shows that the current and permittivity are linked through a truncated form of the Fourier transform.

The dielectric constant for a given frequency depends on the relaxation current around a time corresponding to the reciprocal of the chosen frequency

The above expression implies that the dielectric constant for a given frequency depends on the depolarization current from zero to infinity. It is intuitive however, that the current for a short elapsed time is strongly linked with the permittivity at high frequencies, while the value of the current for longer times reflects the permittivity behavior at lower frequencies. This point will be brought up later.

Experimental determination of a distribution of relaxation frequencies

The determination of a distribution of relaxation frequencies from the experimental depolarization current measurements has been studied by Kliem, Fuhrmann, and Arlt.¹⁰ Their numerical method started from an assumed spectrum on a logarithmic scale of frequency. This spectrum was then adjusted based on a comparison between the data calculated using the assumed spectrum and the measured data. Their method was demonstrated to be suitable both for broad and for narrow spectra of distribution of relaxation frequencies.

Similar methods have also been used in other works but on noise-free data. Other methods also exist but they aim at determining the total response as a combination of discrete number of relaxation frequencies.¹¹

This paper presents, in its first part, a suitable theory for the determination of a distribution function of relaxation frequencies, discussing its various implications on the interpretation of dielectric relaxation phenomena. A second part aims at, using the latter theory, determining numerically the distribution from experimental depolarization current data.

THEORY

Distribution functions

We now assume that the polarization due to a particular dipole moment relaxes according to a distribution of elementary Debye relaxation frequencies $f(\nu)$. In this case the modulus of the change in polarization (i.e., the current) will be given by [see Eq. (2)]

$$\begin{aligned} \frac{d}{dt} P(t) &= I(t) = \int_0^{\infty} \nu f(\nu) P_0 \exp(-\nu t) d\nu \\ &= \int_0^{\infty} F(\nu) P_0 \exp(-\nu t) d\nu, \end{aligned} \quad (8)$$

where use was made of $\nu f(\nu) = F(\nu)$. The function $f(\nu)$ is normalized so that

$$\int_0^{\infty} f(\nu) d\nu = 1. \quad (9)$$

Activation energy and relaxation frequency distribution functions

A relationship exists, which has been described earlier, between a distribution of relaxation frequencies we are looking for and that of activation energies.¹⁰ This will be outlined now. It is often found that the relaxation frequency follows a relationship such as

$$\nu = \nu_{\infty} \exp(-E_a/kT), \quad (10)$$

where ν_{∞} is the so-called infinite relaxation frequency, E_a is the activation energy, k is the Boltzmann constant, and T is the absolute temperature. It should be pointed out that for an isothermal measurement Eq. (10) includes the Arrhenius, the Eyring, and the Williams-Landel-Ferry (WLF) equations. For the WLF equation however, the temperature T has to be substituted by a so-called effective temperature T_e .

It is clear that, whenever such an expression as Eq. (10) holds, a distribution in the activation energies will have as a consequence a distribution of relaxation frequencies. If we denote $g(E_a)$ as the distribution function of the activation energies and using the normalization criterion [i.e., Eq. (9)] we arrive at the following equation relating both distribution functions:

$$\nu f(\nu) = F(\nu) = kTg[E_a = kT \ln(\nu/\nu_0)], \quad (11)$$

provided that the integral of $f(\nu)$ beyond ν_{∞} is very small, which constitutes a very reasonable assumption. In order to make the significance of this equation clearer to the reader, we change the variables ν and t in Eq. (8) by their logarithms, i.e., $\tilde{\nu} = \ln(\nu)$ and $\tilde{t} = \ln(t)$. (Note: throughout this paper a tilde over a variable denotes the *natural logarithm of the variable*):

$$I(t) = \int_{-\infty}^{+\infty} P_0 F(\tilde{\nu}) \exp[\tilde{\nu} - \exp(\tilde{\nu} + \tilde{t})] d\tilde{\nu}. \quad (12)$$

The current for time t is now the integral of the product of $F(\tilde{\nu})$ with a function which depends on the logarithm of the relaxation frequency and on the elapsed time. The function $F(\tilde{\nu})$ has the meaning of the distribution of relaxation fre-

quencies when expressed on a logarithmic scale of frequency. This can be readily demonstrated using the normalization equation [i.e., Eq. (9)] by the change of variable $\tilde{\nu} = \ln(\nu)$.

Using Eq. (11) one now finds a simple relationship between $F(\tilde{\nu})$ and $g(E_a)$,

$$F(\tilde{\nu}) = kTg(E_a) = kTg(kT\tilde{\nu}_{\infty} - kT\tilde{\nu}), \quad (13)$$

which means that the function $F(\tilde{\nu})$ has the same form as that of the distribution of the activation energies, when plotted on a logarithmic scale of frequency.

Mean and standard deviation of the distributions

Using this latter equality [i.e., Eq. (13)] one can easily deduce that when the mean of the $g(E_a)$ is \bar{E}_a that of the function $F(\tilde{\nu})$ will be

$$\bar{\tilde{\nu}} = \tilde{\nu}_{\infty} - \bar{E}_a/kT, \quad (14a)$$

as should be expected. Moreover, with respect to the standard deviations of these density distribution functions it can be deduced that

$$\sigma_{\tilde{\nu}} = \frac{\sigma_{E_a}}{kT}. \quad (14b)$$

These relations mean that as the temperature is raised the mean of the distribution of relaxation frequencies shifts to higher frequencies, while its width narrows and its maximum increases. These conclusions apply provided that the distribution of the activation energies remains constant with temperature. It should be pointed out that a standard deviation of one decade in the distribution of relaxation frequencies corresponds in the activation energy domain to a standard deviation of just 0.06 eV at room temperature.

Time domain measurements

The product time/current and its derivatives

We now multiply both members of Eq. (12) by time t to get

$$I(t)t = \int_{-\infty}^{+\infty} P_0 F(\tilde{\nu}) \exp[\tilde{\nu} + \tilde{t} - \exp(\tilde{\nu} + \tilde{t})] d\tilde{\nu}. \quad (15)$$

This is a very important expression because it tells us that the product of the current by the time is proportional to the convolution of two functions. One which reflects the distribution of the relaxation frequencies [i.e., $F(\tilde{\nu})$] and the other, that will be called temporal-weight function W_t , which is plotted in Fig. 1,

$$W_t(x) = \exp[-x - \exp(-x)]. \quad (16)$$

This function has an asymmetric bell shape with its maximum located at $x=0$ (i.e., $\tilde{\nu} = -\tilde{t}$), while its integral is equal to unity.

From Fig. 1 it is now readily understood the way in which an isothermal depolarization current proceeds in time. For a given time, for example ($t=1$ s; $\tilde{t}=0$), the It product is equal to the integral of the shaded part which reflects the distribution of relaxation frequencies around 1 Hz weighted according to the temporal weight function $W_t(-\tilde{\nu})$. As time

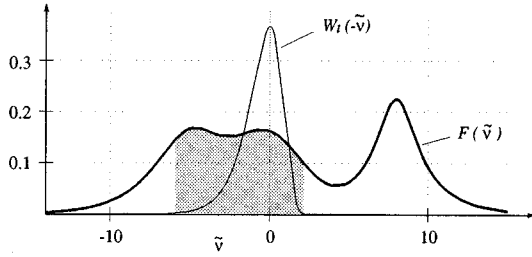


FIG. 1. Location of the temporal weight function $W(t)(\tilde{\nu})$ when $t = 1$ s (i.e., $\tilde{t} = 0$). As time progresses the weight function will slide to the left of the graph.

progresses the function W_t will slide to the left thus probing the distribution function at lower frequencies.

It is interesting to note that a similar expression to that of Eq. (15) is obtained if, instead of the current, one deals with its time derivative. If that case multiplying both members of the resulting equation by t^2 , one gets an expression that involves a convolution of $F(\tilde{\nu})$ with another function, that in this case will be

$$W_t^{(2)} = \exp[-2x - \exp(-x)]. \quad (17)$$

Application to the KWW relaxation function

It is also interesting to mention what one gets when the KWW function is multiplied by the time:

$$It = P_0 \beta_k \exp\{\beta_k(\tilde{\nu}_k + \tilde{t}) - \exp[\beta_k(\tilde{\nu}_k + \tilde{t})]\}. \quad (18)$$

This expression has the same form as that of Eq. (16) but now its width will be a function of the value of β_k . The fact that β_k can only take values from zero to one indicates that this function will always be of equal width or wider than the temporal weight function W_t . For the particular case of β_k equal to one, the Debye relaxation behavior is recovered and this will correspond according to Eq. (15) to a Dirac distribution of relaxation frequencies at the frequency $\tilde{\nu}_k$.

Frequency domain measurements

The relationship between the distribution of relaxation frequencies and permittivity

Similar arguments can be applied in the frequency domain, in line with those in the time domain. When there is a distribution of elementary Debye relaxation frequencies $f(\nu)$ the imaginary and real parts of the permittivity are given, respectively, by²

$$\epsilon''(\omega) = \int_0^\infty \epsilon_s \frac{\omega/\nu}{1 + (\omega/\nu)^2} f(\nu) d\nu, \quad (19)$$

$$\epsilon'(\omega) - \epsilon_\infty = \int_0^\infty \epsilon_s \frac{1}{1 + (\omega/\nu)^2} f(\nu) d\nu. \quad (20)$$

If one replaces the variables ω and ν by their logarithms one gets for the imaginary part

$$\epsilon''(\omega) = \int_{-\infty}^{+\infty} \epsilon_s F(\tilde{\nu}) \frac{1}{2} \operatorname{sech}(\tilde{\omega} - \tilde{\nu}) d\tilde{\nu}, \quad (21)$$

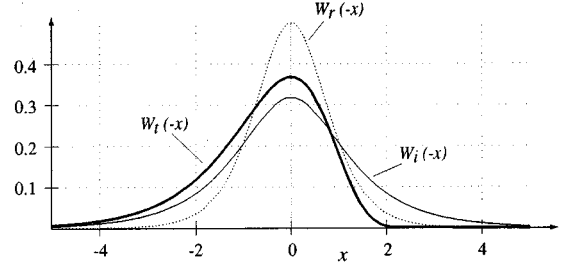


FIG. 2. Normalized weight functions for the It product (W_t), the derivative real (W_r), and imaginary part (W_i) of permittivity.

from which one can appreciate that now the convolution takes place between the distribution function $F(\tilde{\nu})$ and the hyperbolic secant. This latter function is the frequency-weight function W_i as depicted in Fig. 2.

For the real part it is more convenient to deal with its derivative with respect to the logarithm of angular frequency,

$$\frac{d\epsilon'}{d\tilde{\omega}}(\omega) = - \int_{-\infty}^{+\infty} \epsilon_s F(\tilde{\nu}) \frac{1}{2} \operatorname{sech}^2(\tilde{\omega} - \tilde{\nu}) d\tilde{\nu}. \quad (22)$$

In this case the frequency weight function W_r is proportional to the square of the hyperbolic secant (see Fig. 2). In Table I the integral, the mean, and the standard deviation of these weight functions are listed.

Relaxation usually is a step in ϵ' and a peak in ϵ''

It is now easy to observe that a peak in the imaginary part of the permittivity that could, for example, be associated to a peak of the distribution function $F(\tilde{\nu})$, will most probably be associated to a peak in the derivative of its real part because of the similarity of the frequency weight function of these two quantities. As a maximum in the derivative of a function implies an inflexion point in the value of that function we conclude that a peak in the imaginary permittivity will usually be associated to an inflexion point in the curve of the real part of the permittivity.

Scaling and master curves

It is usual to refer to a scaling property of the imaginary part of the permittivity. This consists of adimensionalizing a set of curves taken at different temperatures, plotted on a logarithmic frequency scale, relative to an identifiable point in the curves which can be that of a peak in the imaginary part of permittivity. Using this process a master curve for the permittivity is then obtained.

Within the framework of the above theory [i.e., Eq. (21)], and as long as the relaxation strength of the dipole moment remains constant with temperature, the width of the peaks of

TABLE I. Integral, mean, and standard deviations of the weight functions.

	$\int_{-\infty}^{+\infty} f(x) dx$	\bar{x}	σ_x
W_t	1	-0.577 22	1.2825
W_i	$\pi/2$	0	1.9687
W_r	1	0	0.9069

TABLE II. Examples of distribution functions applicable to relaxation processes.

	$f(u) = f(\tilde{\nu}_m - \tilde{\nu})$	Obs.	$\tilde{\nu}_m^a$	β^a
Cole-Cole, $C(\tilde{\nu})$	$\frac{\sin(\beta_c \pi)}{2\pi[\cosh(\beta_c u) + \cos(\beta_c \pi)]}$	$0 < \beta_c \leq 1$	-5	0.5
Wagner, $W(\tilde{\nu})$	$\frac{1}{\sqrt{2\pi}\beta_w} \exp\left[-\left(\frac{u}{\beta_w}\right)^2\right]$	$\beta_w > 0$	0	3
Fuoss-Kirkwood, $K(\tilde{\nu})$	$\frac{\beta_{fk} \cos(\beta_{fk} \pi/2) \cosh(\beta_{fk} u)}{\pi[\cos^2(\beta_{fk} \pi/2) + \sinh^2(\beta_{fk} u)]}$	$0 < \beta_{fk} \leq 1$	8	0.5

^aParameters used in Fig. 3.

the imaginary part of permittivity will depend on both the width of the hyperbolic secant and on that of the distribution function. As the temperature is raised the standard deviation of the distribution function will be reduced [i.e., Eq. (14b)] as we have realized above. Consequently, a contraction of the peak of the imaginary part of permittivity will be observed. This will make impossible the scaling property *unless* the temperature variation between the curves is not too great. The scaling property however, will in general be apparent if each of the curves is divided by kT prior to their adimensionalization [see Eqs. (13) and (21)].

Hamon approximation

The Hamon approximation^{2,12} is a very effective and simple way to calculate the imaginary part of permittivity from isothermal depolarization current data,

$$\epsilon''(\omega) \approx \frac{1}{\omega} \frac{I(t)}{C_0 V_0}, \quad \omega t = \frac{\pi}{5} = 0.62832. \quad (23)$$

Here, it should be emphasized that the Hamon approximation has implicitly built in the property that the values of the current for short times are linked to the high-frequency spectra of the permittivity and vice versa for the long-time current values.

Using the above theory, namely, Eqs. (4b), (15), and (21), we arrive at the conclusion that the imaginary part of the permittivity is related to the measured current through

$$\epsilon''(\omega) \approx 0.8819 \frac{1}{\omega} \frac{I(t)}{C_0 V_0}, \quad \omega t = 0.56146. \quad (24)$$

This relationship was obtained using the following reasoning: both quantities (i.e., the It product and the imaginary part of permittivity) are an average of the distribution function weighted according to two different functions, W_i and W_j . If the mean values of these functions are made to coincide in such a way that their bell shapes overlap each other in the same part of the distribution spectrum, then the relation of Eq. (24) follows.

It is apparent that the Hamon approximation [i.e., Eq. (23)] and Eq. (24) are quite similar. This enables us to understand better why the Hamon approximation has been so successful in the past. In fact to deduce Eq. (24) we have not assumed any distribution at all and thus the Hamon approximation is a quite general one, independent of the distribution function and/or on the form of the depolarization current. It

is apparent, however, that the smoother the distribution function is the closer the approximation will be.

A similar result can be deduced relating the current to the derivative of the real part of permittivity,

$$\frac{d\epsilon'(\omega)}{d\omega} \approx -0.56146 \frac{1}{\omega} \frac{I(t)}{C_0 V_0} \approx -\frac{2}{\pi} \epsilon''(\omega),$$

$$\omega t = 0.56146. \quad (25)$$

Theoretical distribution functions: Wagner, Cole-Cole, and Fuoss-Kirkwood

Some distribution functions have been proposed before, where most of them were deduced from proposed theoretical permittivity curves. Examples of these distributions are the Cole-Cole, the Fuoss-Kirkwood, the Wagner, as well as the Davidson-Cole and the Havriliak-Negami distribution functions.³ The first three have been selected in this paper as working theoretical distribution models and they are listed in Table II and plotted in Fig. 3. They have in common the facts (1) of being distribution functions on a logarithmic scale of frequency, (2) of showing a symmetrical bell shape around a mean frequency (i.e., $\tilde{\nu}_m$) and finally, (3) the existence of a parameter (i.e., β) which controls the width of the distribution function.

Deconvolution method

General method

After defining a suitable relation between the current and the distribution function through Eq. (15) it is necessary to devise a way to extract the distribution of relaxation frequencies from the experimental isothermal depolarization current

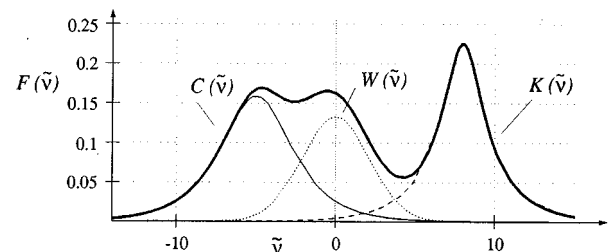


FIG. 3. Examples of distribution functions. Curves C , W , and K represent a Cole-Cole, a Wagner, and a Fuoss-Kirkwood distribution, respectively. Refer to Table II for values of the parameters used in the graph.

data. This is best accomplished using an *iterative* method akin to that used by Kliem, Fuhrmann, and Arlt¹⁰ after suitable modifications. The steps taken for this effect are as follows:

- step 1: Determine the experimental time/current product and condition the data file,
- step 2: perform a first estimate of the distribution of relaxation frequencies,
- step 3: eliminate noise from the distribution function and extend the data window,
- step 4: calculate the current,
- step 5: determine correction factors eliminating noise,
- step 6: *determine a new distribution function*,
- step 7: go to step 4 until error in the current computed from the distribution function relative to the measured current does not improve significantly,
- step 8: calculate the permittivity.

A further description of the more important of the above steps will now be provided.

Step 1: Determine the experimental time/current product and condition the data file

In order to obtain the experimental current one has first to polarize the sample during a time t_p much longer than the time t_f during which the depolarization current will be recorded. Because of the finite time response of the measuring devices the monitoring of the current will begin at time t_i and be stopped at t_f thus setting the *data window* for the experiment. *The aim in the subsequent steps will be the determination of the distribution of relaxation frequencies within the window defined around the interval $[1/t_f, 1/t_i]$.*

The ideal way to monitor the current would be to sample the current logarithmically spaced in time. As this is not practical in many cases we propose here to sample linearly within each time decade. After completing the experiment a *vector* for the measured It product can then be created using a logarithmic interpolation, with time increasing logarithmically. The number of points of the new vector should be the same as that of the experimental vector.

The number of experimental points within each decade sets the resolution for the determination of the distribution function. A reasonable number has been found to be between 20 and 30 points per decade.

It should be noticed here that in a real experiment the quantity one is looking for is $\epsilon_s F(\bar{\nu})$ and not $F(\bar{\nu})$. The former quantity is the product of the relaxation strength of the dipole moment and a distribution function. To this effect Eq. (15) must be rewritten using Eq. (4b) thus,

$$\frac{It}{C_0 V_0}(\bar{t}) = \int_{-\infty}^{+\infty} \epsilon_s F(\bar{\nu}) \exp[\bar{\nu} + \bar{t} - \exp(\bar{\nu} + \bar{t})] d\bar{\nu}. \quad (26)$$

As the integral of the distribution function is equal to one, the integral of the product $F_\epsilon = \epsilon_s F(\bar{\nu})$ will equal the relaxation strength of the dipole moment.

Step 2: First estimate of the distribution of relaxation frequencies

Given a frequency ν we must now estimate the distribution function at that frequency. In view of the fact that the It product at time t reflects a local average of the distribution

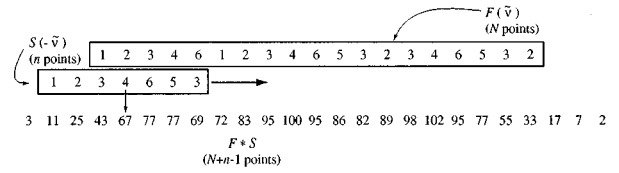


FIG. 4. Schematic of a serial multiplication of vectors.

function around $\bar{\nu} = -\bar{t}$ (see Fig. 1) it is reasonable to assume that the value for the distribution function at frequency ν is approximately

$$F_\epsilon(\bar{\nu}) \approx \frac{It}{C_0 V_0} (\bar{t} = -\bar{\nu}). \quad (27)$$

Thus, for example, the current measured at $t = 1$ s (i.e., $\bar{t} = 0$) will thus reflect the value of the distribution function around the frequency of $\nu = 1$ Hz (i.e., $\bar{\nu} = 0$). This argument also implies that for a time window of $[t_i, t_f]$ the corresponding frequency window, for the distribution function, will be $\bar{\nu} = [-\bar{t}_f, -\bar{t}_i]$.

Considering the experimental It product as a vector of length N , arranged in reversed order (i.e., from long to short times) one has

$$F_{\epsilon i}^0 = \frac{It_i}{C_0 V_0} = It_i^r, \quad (28)$$

where i refers to the i th point from the appropriate vectors. F_ϵ^0 will then be a vector arranged from low to high frequency.

Steps 3 & 4: Eliminate noise from the distribution function and extend the data window. Calculate the current from estimated distribution function

This is a critical step. In the past, the existence of noise in the measured data has prevented the deconvolution process due to the numerical instabilities it creates. In fact what is needed is a method of smoothing the estimated distribution function while retaining its main features. Various methods have been proposed in the literature to this end. The one used in the present work, which was found to be quite simple and effective, resorts to a convolution process between the estimated distribution function and a smoothing function S .

It is pointed out now that the calculation of the It product [see Eq. (26)] using the estimated distribution function also involves a convolution between two functions, namely, the estimated distribution function and the temporal weight function. Steps 3 and 4 have thus some common features and they will be approached together. The convolution of two vectors, of which the two above cases are examples, can be performed through a technique called serial multiplication¹³ that is schematically shown in Fig. 4.

The idea is to write the vectors to be convoluted onto two strips of paper, one of them written in reverse order. The convolution vector is then obtained by sliding one strip of paper over the other while adding up the product of corresponding numbers as shown in Fig. 4.

Thus, to calculate the It product a vector was created for the temporal weight function with the same spacing as that

of the estimated distribution function, centered at zero and whose frequency range was on a natural logarithmic scale $[-6.91, 6.91]$. It was found that this frequency range provided a good precision in the calculation of the It product. The number of points n was chosen to be an odd number, so that the maximum (i.e., $\tilde{\nu}=0$) would be at the center of the vector.

The smoothing vector S was chosen to be a Gaussian with its maximum lying in the middle of the vector and its role is to smooth out the noise in the estimated distribution function. The length of this smoothing vector was chosen to be the same as that of the temporal weight vector (i.e., n). The standard deviation of the Gaussian was usually of one unit, in a natural logarithmic frequency scale. A larger or smaller standard deviation could also be used depending on the noise in the data.

The above smoothing operation of the estimated distribution vector, as it is, would not work properly at the edges of the estimated distribution vector (see Fig. 4). The reason is that the smoothing operation is a kind of average of neighboring points weighted according to the smoothing vector with the latter having the property that the sum of its points is equal to unity. As one approaches the edges however, it should be realized that the strip of paper in Fig. 4 corresponding to the estimated distribution vector will not contain the smoothing vector completely and thus one must take into consideration that the average is taken with fewer and fewer points. Thus, a vector W_s was created equal to the convolution of the smoothing vector S with a unit vector whose length was the same as the estimated distribution vector (i.e., N). The vector W_s is then a kind of integral of the weights used in the smoothing operation. The resulting smoothed distribution vector was then divided by the vector W_s in order to take this effect into consideration. Finally, if N is the number of points of the estimated distribution function and n is the length of the S vector then the total number of points after the smoothing operation will be equal to $N+n-1$.

$$\text{Step 3: } F_{\epsilon}^1 = \frac{S * F_{\epsilon}^0}{W_s}. \quad (29)$$

A related problem arises in step 4 to calculate the It product from the estimated distribution vector. Near the edges and in order to calculate the It product some extension of the distribution function beyond the data window must be made.

This extended distribution vector was chosen to be precisely the one which resulted from the smoothing operation which as was pointed out has extended the distribution vector from N to $N+n-1$ points. The calculation of the It product proceeded through the convolution of the extended distribution vector with temporal weight vector multiplied by the logarithmic frequency spacing.

$$\text{Step 4: } It^k = F_{\epsilon}^k * (W_t \cdot \Delta \tilde{\nu}), \quad (30)$$

where k refers to the k th iteration. From the resulting It vector only the N central points were then selected as those corresponding to the experimental It product.

Steps 5 & 6: Determine correction factors and a new distribution function

In this step the computed product It^k from the last step is compared with the experimental vector It^r to determine the so-called correction factors

$$\text{Step 5: } q_i^k = \frac{It_i^r}{It_i^k}. \quad (31)$$

Vector q^k , of length N and whose values are centered around one, is then smoothed according to the same procedure used for the first estimate of the distribution. The smoothing, however, was performed over q^k-1 . The values of q^k were recovered afterwards by adding one. We thus obtain an extended smoothed vector Q^k of length $N+n-1$:

$$\text{Step 5: } Q^k = 1 + \frac{(1 - q^k) * S}{W_s}. \quad (32)$$

A new extended distribution vector is then computed using

$$\text{Step 6: } F_{\epsilon i}^{k+1} = Q_i^k F_{\epsilon i}^k. \quad (33)$$

This procedure which resembles that used by Kliem, Fuhrmann, and Arlt¹⁰ proved to be convergent to the proper values of the distribution function throughout our work. It is also a fast and simple algorithm although its mathematical justification has not been found.

Step 7

Go to step 4, until error in the It product computed from the distribution function relative to the measured It product does not improve significantly. The error was calculated as the standard deviation of the difference of the two vectors.

Step 8: Calculate the permittivity

After obtaining the distribution function, the imaginary part of the permittivity can be calculated using Eq. (21) and a serial multiplication procedure. From Eqs. (21) and (22) it can be realized that the angular frequency data window for the permittivity will be equal to the frequency window of the distribution function so that one has $\tilde{\omega} = [-\tilde{t}_f, -\tilde{t}_i]$. Consequently the frequency window for the permittivity will be

$$\tilde{f} = [-\tilde{t}_f - \ln(2\pi), -\tilde{t}_i - \ln(2\pi)]. \quad (34)$$

To calculate the real part of permittivity its derivative must be first computed from Eq. (22). Its value, less an arbitrary constant, can then be estimated through an integration operation. These values for the imaginary and real part of the permittivity can then be compared with those obtained using the Hamon approximation or Eqs. (24) and (25).

RESULTS AND DISCUSSION

Two sets of tests for the above deconvolution procedure were carried out.

(1) A distribution function consisting of a combination of theoretical distribution functions has been used as the basis for the calculations.

(2) A comparison with previous results using the data

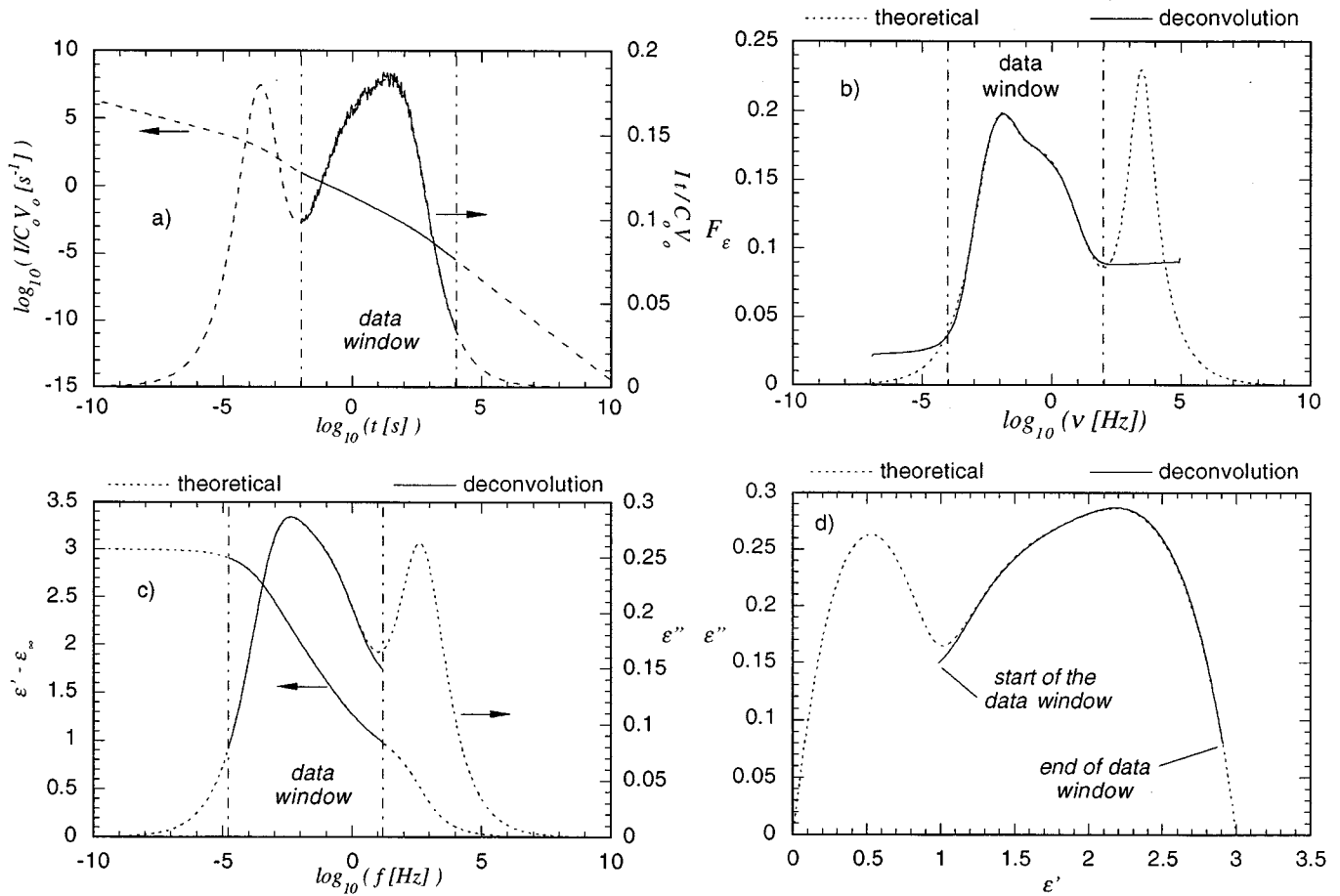


FIG. 5. Graphs produced using a theoretical distribution function of relaxation frequencies.

from Kliem, Fuhrmann, and Arlt¹⁰ and those of Mopsik¹⁴ was also performed.

Determination of the distribution function from simulated current spectra

The theoretical distribution used in this test is the one plotted in Fig. 3. It consists of a combination of a Wagner, a Cole-Cole, and a Fuoss-Kirkwood distribution, with relaxation strengths equal to one, and whose other parameters are the same listed in Table II.

The resulting It product is plotted in Fig. 5(a) and was calculated using Eq. (26) and a serial multiplication procedure with 20 points per decade of frequency. It should be noted that, in this phase, the length of the temporal weight vector used for convolution was made equal to that of the distribution function. Using the It product the current was then calculated [Fig. 5(a)]. The current vector was afterwards clipped between $t=10^{-2}$ s and $t=10^4$ s and a 5% error incorporated into it.

This simulated current vector was then introduced into the deconvolution program to determine the distribution of relaxation frequencies [Fig. 5(b)], the imaginary and real part of permittivity [Fig. 5(c)], as well as the Cole-Cole plot of these latter quantities [Fig. 5(d)]. The real part of permittivity

acquired from the deconvolution procedure was obtained using an arbitrary constant which was taken from the theoretical curve.

As can be noted from Fig. 5(b), the error between the simulated distribution function and that resulting from the deconvolution procedure is quite low inside the data window. Clipping at $t=10^{-2}$ s as was done in the present example is an unfavorable situation in terms of extending the data window into higher relaxation frequencies and consequently there is a significant error in the extension into this region of the frequency spectrum. This problem would be of no consequence if we were only interested on the distribution of relaxation frequencies. On calculating the permittivity, however, this extension will have implications especially on those frequencies closer to the edges of the data window. The degree of impact of the assumed extension will be greater in the case of the imaginary part of the permittivity, which has a weight function of a large width, than for the real part of permittivity, with a weight function that has the smallest of widths among the weight functions (see Fig. 2 and Table I). Consequently for the real part hardly any error can be noticed in this case and indeed in most cases.

The choice of the smoothing function must be based both on the noise present on the It product and on the frequency resolution, each of them imposing conflicting requirements

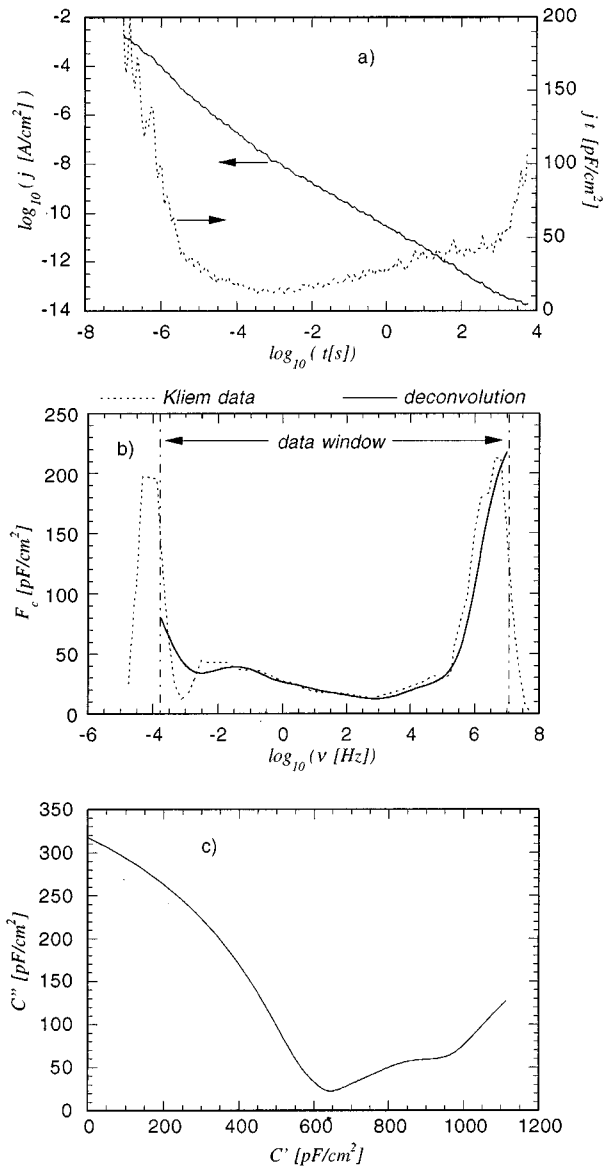


FIG. 6. Test and comparisons using data from Kleim, Fuhrmann, and Arlt (Ref. 10), (a) current and It product, (b) distribution function of relaxation frequencies, and (c) Cole-Cole plot for the permittivity.

over it. A broad smoothing function, for example, will eliminate a large noise but it will also smear sharp peaks present in the distribution function. The standard deviation of the Gaussian smoothing function must be therefore as small as possible compatible with the noise present in the data. Finally, it should be mentioned that the deconvolution is in general a quite fast procedure. For the example presented here ten iterations had to be performed until the error in the It product did not reduce between iterations by more than 5% and these iterations implemented using MATLAB® took a 486 PC only about a minute of execution time.

COMPARISON WITH PREVIOUS RESULTS: MOPSIK AND KLIEM

Kliem measurements of the distribution function

Data from the paper by Kliem, Fuhrmann, and Arlt¹⁰ were used in order to compare the distribution function they ob-

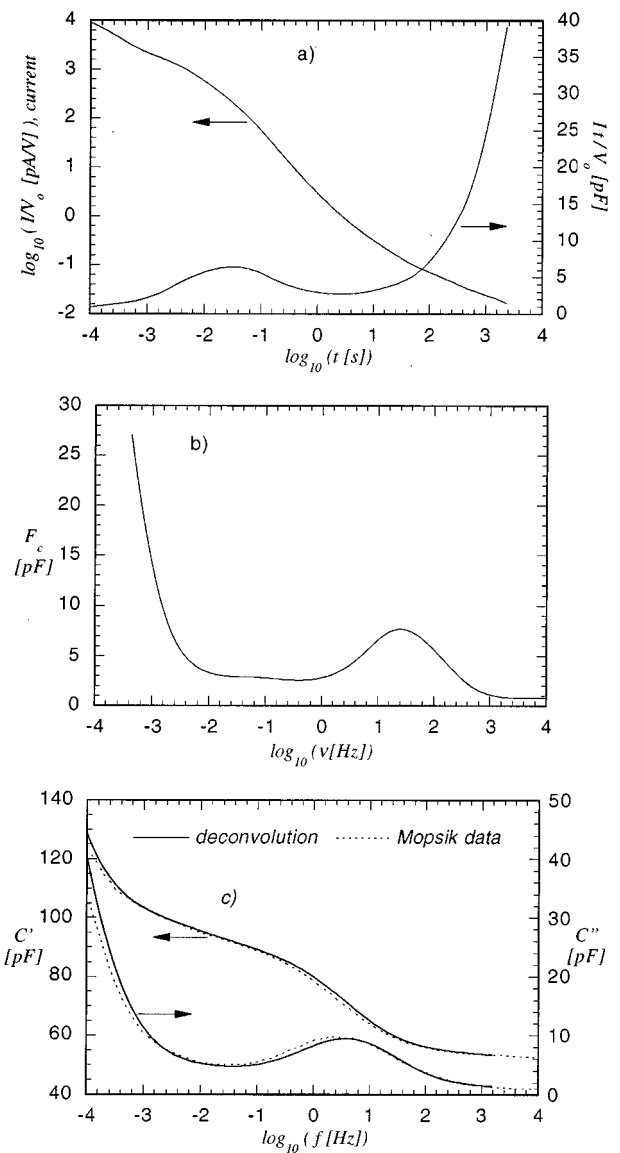


FIG. 7. Test and comparisons using data from Mopsik (Ref. 14), (a) current and It product, (b) distribution function of relaxation frequencies, and (c) real and imaginary part of permittivity.

tained and the one resulting from the above deconvolution procedure. In Fig. 6(a) is shown the current density that was measured for dried polyimide over 11 decades on a logarithmic scale of time. The results for the distribution function quoted in that paper are shown in Fig. 6(b). Based on these findings the authors pointed out the existence of two relaxations, one in the region $10^6 \leq v \leq 10^7$ and the other $v \approx 10^{-4}$ Hz.

In Fig. 6(a) is also shown the It product calculated for that experiment, from which can be observed an indication of relaxations on both extremes of the data window. Based on the It product a deconvolution was undertaken to determine the distribution function which is plotted in Fig. 6(b). It can be noticed that although not coincident both curves do agree in general. It is apparent, furthermore, that a small relaxation in the region of 3×10^{-2} Hz also exists, which can be appreciated from Fig. 6(c) representing the Cole-Cole plot of the permittivity. In the latter graph the arbitrary constant of the real part of permittivity was set equal to zero.

Mopsik data for dielectric measurements

Mopsik has developed a method to calculate the permittivity from the measured time-dependent capacitance during charging of a sample. This method is based on splines in order to perform the Fourier transform of the current of Eq. (7).⁹

From the time-dependent capacitance quoted in that article the current for each unit of the applied voltage was calculated which is shown in Fig. 7(a) together with the corresponding It product. Using the deconvolution procedure the distribution function was calculated that is shown in Fig. 7(b), where it can be observed that a relaxation exists near 25 Hz. It is also apparent that in the low-frequency end the distribution shows a very large increase. This can be due to the fact that the experiment was performed while charging a sample. When the time during charging is large enough, so that the current begins to stabilize near its dc value, the distribution function will tend to behave as it does in this case. From Eq. (26) one can indeed conclude that if the current is constant in time then the distribution function will have to increase as the frequency decreases.

From the distribution function the real and the imaginary parts have been calculated and compared with those of the Mopsik article [Fig. 7(c)]. The arbitrary constant for the real part of permittivity was found so that the correspondent curves would coincide at the start of the data window.

From the analysis of Fig. 7(c) one can observe that both the real and the imaginary part of the permittivity coincide between these two methods. The observed discrepancy could be attributed both to errors in the digitalization of the time-dependent capacitance and/or to the following calculation of its time derivative in order to calculate the current.

FINAL REMARKS

The It product

A new general approach has been presented for the determination of the distribution of relaxation frequencies from depolarization data. In this approach the It product was shown to play a pivotal role. Interestingly, this quantity is equal to the time derivative of polarization with respect to the natural logarithm of time,

$$\frac{dP}{d\ln t} = It. \quad (35)$$

This quantity has been recognized since the work of Hamon and others to have special properties, namely, in regard to the calculation of the imaginary part of permittivity from depolarization data.^{2,15,16} Its importance lies in the demonstration that for a given time its value corresponds to a weighted average of the distribution of relaxation frequencies around $1/t$. It was moreover demonstrated that the weight function has an asymmetrical bell shape whose mathematical expression is given by Eq. (16).

The basic premise in the theory however, is that the natural scale for the distribution function of relaxation frequencies is logarithmic in the frequency axis. This property follows if there is both a distribution of activation energies of the relaxing dipole moment and if the relationship between

the activation energy and the relaxation frequency is of an exponential type like in an Arrhenius equation.

The width of the distribution function

The width of the distribution function has been shown to be temperature dependent through Eq. (14b). That equation, although simple in formulation, is of a fundamental importance. It states that if the distribution in the activation energies remains constant, as the temperature increases the distribution in the relaxation frequencies, on a logarithmic scale, tends to shrink. This is a common finding in the literature regarding the plots of the imaginary part of permittivity.² Based on that equation, a conjecture can also be enunciated regarding the width of the distribution of relaxation frequencies for a given temperature. Given two distributions in the activation energies the one with a higher mean value will generally have a lower relaxation frequency. If we suppose that the standard deviation increases with the mean energy, then polarization mechanisms with a lower relaxation frequencies will tend to show a broader peak both in the imaginary part of permittivity and in the It product. This is what often is observed: the lower the relaxation frequency the broader are the peaks.^{1,2}

The measurement of the distribution function as a function of temperature

The experiments dealt with in this paper were of an isothermal kind. This theory however, when extended to the measurement of the distribution function of relaxation frequencies at various temperatures should enable the determination of some of the characteristics of the distribution of activation energies, through Eq. (13). This topic, that is of the utmost importance because it relates to the basic premise in this paper, will be the subject of future work.

Deconvolution

The deconvolution process proposed here is a very simple and effective procedure. Higher numerical sophistication however, could be used to this end.

For example, after step 7, the new-found distribution could be regarded now as a first estimate of the distribution function, as was first performed with the It product in step 2, and the process of iteration could restart again from step 3, with the advantage of having a better estimate of the distribution both inside and outside of the data window.

This justifies the need of more work regarding (1) a quantitative evaluation of the errors incurred in this deconvolution procedure, (2) the determination of the minimum data window which must be used for the deconvolution procedure, as well as the (3) interrelation between the width of the smoothing function, the number of points N , and the resolution of the deconvolution procedure. The generality of the proposed deconvolution procedure allows, also, its application to the deconvolution of the imaginary permittivity data. The difference is that the relevant weight function would be W_i instead of W_t . This fact opens up the possibility of performing a complete spectroscopy for the distribution func-

tion from very high frequencies down to very low frequencies by conjugating time and frequency domain techniques.

Finally, as a note of caution, it should be stressed that the distribution of relaxation frequencies method is just one possible approach to the phenomena of dielectric polarization, and that alternative explanations and theories exist.¹⁷ There is, indeed, still some fundamental doubts about whether the Debye type of relaxation should be taken as the elementary

block in this theory due to the Kubo restrictions it does not satisfy.

ACKNOWLEDGMENTS

The author is grateful to J. N. Marat-Mendes (UNL-FCT-SGAAF), D. K. Das-Gupta, and T. J. Lewis from University of Wales (SEECs-Bangor-UK) for the helpful and valuable discussions.

¹F. K. Kneubühl, *Infrared Phys.* **29**, 925 (1989).

²N. G. McCrum, B. E. Read, and G. Williams, *Anelastic and Dielectric Effects in Polymer Solids* (Wiley, New York, 1967).

³J. Vanderschüren and J. Gasiot, in *Thermally Stimulated Relaxation in Solids*, edited by P. Bräunlich (Springer-Verlag, Berlin, 1979), p. 154.

⁴J. R. MacDonald, *J. Appl. Phys.* **62**(11), R51 (1987).

⁵G. Williams and D. C. Watts, *Trans. Faraday Soc.* **66**, 80 (1970).

⁶F. Alvarez, A. Alegria, and J. Colmenero, *Phys. Rev. B* **47**, 125 (1993).

⁷R. Kubo, *Rep. Prog. Phys.* **29**, 255 (1966).

⁸R. Lovell, *J. Phys. C* **7**, 4378 (1974).

⁹F. I. Mopsik, *IEEE Trans. Electr. Insul.* **EI-20**(6), 957 (1985).

¹⁰H. Kliem, P. Fuhrmann, and G. Arlt, *IEEE Trans. Electr. Insul.* **23**(6), 919 (1988).

¹¹K. Tittelbach-Helmrich, *Meas. Sci. Technol.* **4**, 1323 (1993).

¹²D. K. Das-Gupta and K. Joyner, *J. Phys. D* **9**, 829 (1976).

¹³R. N. Bracewell, *The Fourier Transform and its Applications* (McGraw-Hill, New York, 1986).

¹⁴F. I. Mopsik, *Rev. Sci. Instrum.* **55**(1), 79 (1984).

¹⁵T. J. Lewis, in *Dielectric and Related Molecular Processes*, edited by M. Davis (The Chemical Society, London, 1977), pp. 186–218.

¹⁶E. Schlosser and A. Schönhals, *Colloid Polym. Sci.* **267**(11), 963 (1993).

¹⁷A. K. Jonscher, *IEEE Trans. Electr. Insul.* **27**(3), 407 (1992).